Materials and Structures/Matériaux et Constructions, Vol. **30**, June 1997, pp 293-305

Self-desiccation and its importance in concrete technology

Bertil Persson

Lund Institute of Technology, Division of Building Materials, University of Lund, P. O. Box 118, 221 00 Lund, Sweden

A B S T R A C T

In this article, an extensive experimental and numerical study of self-desiccation and its importance in concrete technology is outlined. For this purpose, cubes and cylinders of eight qualities of concrete were studied at 4 different ages for each one. Parallel studies of autogeneous shrinkage, basic creep, hydration, internal relative humidity and strength were carried out. Previous research in the field is summed up. Finally, the article presents the mechanisms of self-desiccation as well as its importance in concrete technology by modelling the autogenous shrinkage and its effect on basic creep. This project was carried out between the years 1992 and 1995.

R É S U M É

Cet article présente une vaste étude expérimentale et numérique sur l'autodessication ; son importance dans la technologie du béton est passée brièvement en revue. Des cubes et des cylindres de huit qualités différentes de béton ont été étudiés, chacun à quatre âges différentes. Des études parallèles ont été menées sur le retrait endogène, le fluage, l'hydratation, l'humidité interne relative et la résistance. Des recherches antérieures dans ce domaine sont résumées. Enfin, l'article présente les mécanismes de l'autodessication et son importance dans la technologie du béton par la modélisation du retrait endogène et de son effet sur le fluage. Ce projet de recherche a été mené entre 1992 et 1995.

1. INTRODUCTION

1.1 Self-desiccation

Self-desiccation has attracted minor interest in previous studies performed on normal concrete [1]. However, for concretes with less water available than required for the hydration process to be completed, self-desiccation is of great interest. The self-desiccation of the concrete was found to be favourable in avoiding moisture damage during the construction period. However, self-desiccation of the concrete also caused an autogenous shrinkage of the concrete which may lead to early cracking [2]. Finally, the basic creep of the concrete, defined as deformations under constant moisture and stable temperature conditions, was also affected by self-desiccation.

1.2 High Performance Concrete

High Performance Concrete, HPC, is a concrete with a 28-day, 100-mm cube compressive strength exceeding 80 MPa; HPC also displays good rheological properties. In a fresh state, it is possible to mix, transport and cast HPC with existing methods. The maximum compressive strength will be about 180 MPa under these conditions. Because such a concrete possesses – in addition to high strength – several other favourable qualities such as low permeability and self-desiccation, a new definition was created: HPC. The ratio of the amount of water to the amount of cement in the concrete, w/C, is larger than 0.38 for normal concrete, while it varies between 0.20 and 0.38 for HPC. The low water-cement ratio requires special additives in the concrete mix, such as silica fume and above all a superplasticizer, to obtain good workability. Most often, low-alkali cements are also required. The type of aggregate is important for obtaining high strength. The grading of the aggregate influences the concrete's workability. The order of mixing the material involved is also important for the workability of the concrete. Several properties of the concrete are heavily related to the water-cement ratio, such as compressive strength, internal relative humidity, hydration and compliance, ε/σ. Other properties such as Young´s modulus, Poisson´s ratio and the creep coefficient do not vary much as compared to normal concrete, since they are mainly dependent on the quality of the aggregate.

Editorial note
Mr. Bertil Persson is a RILEM Senior Member. He participates in TC 161-GMC on Modelling the behaviour of Concrete in service: a Guide for the engineer.

0025-5432/97

1.3 Basic creep

Generally, basic creep includes the deformations related to loading on the concrete at constant ambient climatic conditions (temperature and moisture stability). The ambient temperature must be held constant. The moisture exchange from the concrete to the surroundings must be zero, *i.e.* the weight of the concrete is also constant. The basic creep of HPC includes a phenomenon called "autogenous shrinkage". The autogenous shrinkage of HPC is an effect of its self-desiccation. The self-desiccation of HPC is beneficial in solving problems related to moisture from the concrete during the period of construction. Plastic carpets, which are glued to normal concrete, often loosen due to an excessive moisture content in the concrete. With self-desiccation, the internal relative humidity rapidly decreases below the critical level. Problems related to moulds, etc. in connection with the moisture content in normal concrete are also solved by the use of HPC. The autogenous shrinkage could also be beneficial as it acts in the opposite direction to the temperature expansion during the early hydration. However, the autogenous shrinkage could cause cracking even when the concrete is exposed to water. The low permeability of HPC prevents the water from entering the interior of large structures and thus the self-desiccation might cause cracking due to the autogenous shrinkage. Fig. 1 presents the concept definition for different deformations related to the basic creep of concrete at different ages.

2. OBJECTIVES, LIMITATIONS AND GENERAL LAYOUT OF THE WORK

2.1 Objectives

1) Separation of elastic deformation, plastic and viscous basic creep

To ascertain the amount of elastic deformation, plastic and viscous basic creep of HPC with a water-cement ratio varying between 0.25 and 0.38 by studying both well-hardened concrete and concrete during hydration. The effect of air-entrainment and of different amounts of silica fume additive was to be determined at one specific water-cement ratio only. National concrete mix proportions were to be included in the study.

2) Model of basic creep during hydration

3) Effect of stress/strength ratio (load level) on basic creep

To ascertain the effect of a high stress/strength ratio (load level) for concrete during hydration by studying HPC with a water-cement ratio varying between 0.25 and 0.38. The effect of air-entrainment and of different amounts of silica fume additive was to be determined at one specific water-cement ratio only. National concrete mix proportions were to be included in the study.

2.2 Limitations

1) Long-term stability

The long-term stability was limited to studies of basic creep during a period of 1 year.

2) Autogenous shrinkage

The studies started at 1 day of age and were limited to a period of 2 years. The internal relative humidity was established at 1, 2, 3, 4, 6, 28, 360 and 720 days of age only.

3) Size of specimen, materials, etc.

The specimen size was limited to a diameter of 55.5 mm and a length of 300 mm. The studies of compressive strength were carried out for 100-mm cubes only. The measurement points for deformation were cast in the cylinders. All specimens were membrane-cured by 2-mm vulcanized butyl rubber clothing. Aggregates of crushed quartzite and natural sand of gneiss were used in the standard mix proportions. In the studies, only low-alkali Portland cement was used. In the standard mix proportions, granulated silica fume was used. The air-entrainment varied between 1% and 5%, as calculated for the total volume of the concrete. A superplasticizer based on melamine formaldehyde was added to all mix proportions. In the national mix proportions, silica fume slurry was used together with crushed granite and natural sand based on granite.

2.3 General layout of the work

1) MTS machine studies

Studies of the separation of elastic deformation from viscoelastic and viscoplastic creep were carried out on cylinders in an oil accumulator and in an electronic servo-

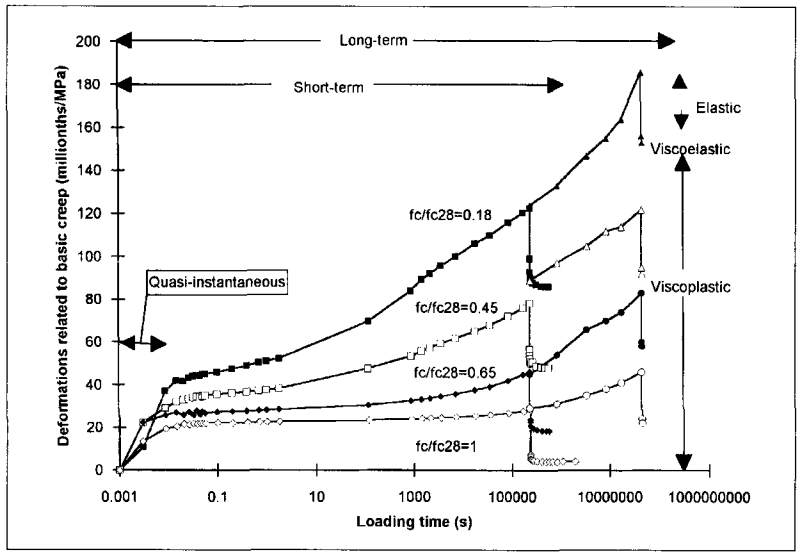

Fig. 1 – Concept definition for various deformations related to the basic creep of concrete at different ages. fc = compressive strength at loading (fc28 = 28-day strength of the concrete).

controlled MTS machine [3]. The deformations were measured by separate LVDT displacement and gauging transducers and collected by a separate computer. The full level of loading was applied within about 0.01 s. At both loading and unloading, the measurements were carried out 3,000 times per second including 3 longitudinal LVDTs and one LVDT placed transversally to the cylinder.

2) Studies in a spring loading device

Long-term stability tests and plastic and viscous creep tests at 1 year of loading duration were conducted on cylinders in a traditional mechanical spring loading device. At all times of measurement, the specified loading of the spring was applied. This loading was applied simultaneously to the loading in the MTS machine. Thus, the quasi-instantaneous loading in the MTS machine was prolonged by studies of creep in the traditional spring device. The weight of the cylinders was established both before and after the studies.

3) Autogenous shrinkage

Studies of autogenous shrinkage on horizontal (lying) cylinders. The cylinders were turned a third of a full turn at each measurement to avoid bending effects. The weight was recorded.

3. MATERIALS, PREPARATION OF SPECIMENS AND PRINCIPAL PROPERTIES

3.1 Materials

The following materials were used for the 6 standard and 2 national mix proportions:

1) Aggregates

The main characteristics of the aggregates are displayed in Table 1 [4].

2) Cement

A low-alkali Portland cement, Degerhamn Standard, was used. The chemical composition and main characteristics of the cement are shown in Table 2.

3) Silica fume

For the standard mix proportion, granulated silica fume was used (ignition losses 2.26% by weight). For the national mix proportions, R, micro silica fume slurry was applied (ignition losses 1.86% by weight).

4) Superplasticizer

For all mix proportions, a superplasticizer was used, based on melamine formaldehyde.

Table 1 – Characteristics of the aggregates

Material/ characteristics	Young´s modulus (GPa)	Compressive strength (MPa)	Split strength (MPa)	Ignition losses by weight (%)
Quartzite sandstone, Hardeberga	60.2	332	15.0	0.28
Natural sand, Åstorp				0.79
Granite, Norrköping	61.2	153	9.6	1.67
Pea gravel, Toresta				1.62
Crushed sand, Bålsta	59.1	234	14.3	1.95

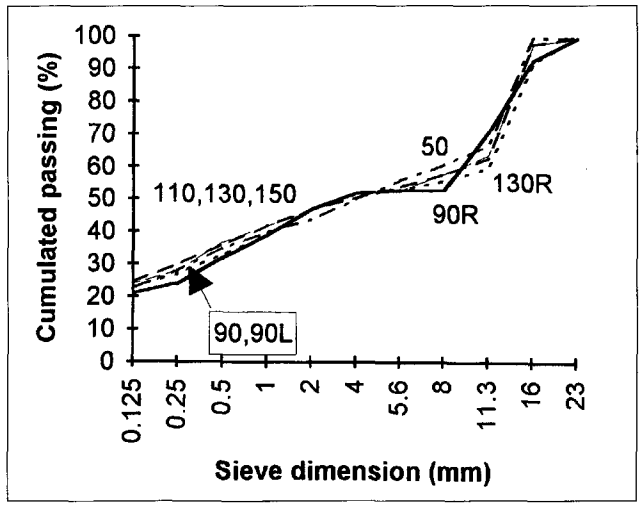

Fig. 2 – Cumulative percentage passing of all the aggregates, cement and silica fume for the different concrete types indicated. The mix proportion is indicated.

5) Air-entrainment agent

Some mix proportions (indicated by L) used an air-entrainment agent based on vinsole resin.

6) Cumulative percentage passing

The cumulative percentage passing for all the aggregates, cement and silica fume, given in Fig. 2, was basically bi-logarithmic between 0.125 mm and $0.7 \cdot D_{max}$ (D_{max} = max. aggregate size).

3.2 Preparation of specimens

1) Material

The aggregates were stored in rubber barrels in order to maintain a moisture content of about 4% by weight. Compensation for the moisture content was made when adding the remaining mixing water. All of the material had a temperature of 20 °C. The mixing of the concrete took place in a 25-l compulsive mixer. At first, all material except for the silica fume slurry (where applicable) and the superplasticizer was mixed for 1/2 minute. The superplasticizer and the silica fume slurry (mix proportions R) were then added and the mixing continued for another 2 1/2 minutes.

Table 2 – Chemical composition and main characteristics of the cement

Property	Composition or characteristics
CaO	64.9%
SiO_2	22.2%
Al_2O_3	3.36%
Fe_2O_3	4.78%
MgO	0.91%
K_2O	0.56%
Na_2O	0.04%
SO_3	2.00%
Ignition losses	0.63%
Specific surface acc. to Blaine	302 m^2/kg
Density	3220 kg/m^3

2) Moulds

The circular moulds had an inner diameter of 55.5 mm and a length of 300 mm. Six cast-in items were placed 25 mm from the ends of the mould and 2 items were positioned on opposite sides at the middle of the mould. The items were fixed by 3-mm bolts through the steel. The cast-in items all had a diameter of 8 mm and a depth of 16 mm. They were provided with flanges and edged to avoid movement in the concrete. The cube moulds were also made of steel. Thermocouples were cast in one cylinder and in one cube out of each batch.

3) Casting

After measuring air-entrainment and density, the moulds were filled up under vibration. The cylinders were levelled off at the upper end. A 10 mm steel plate was fixed and vibrated to the end of the cylinder horizontally (lying down). The ends of the cylinder were smooth; grinding was not necessary. All specimens were then placed in a rubber container to avoid loss of moisture. (The moisture absorption in the rubber between an ambient relative humidity of ϕ = 65% and ϕ = 95% was hardly detectable, *e.g.* less than 1 per mil compared to the weight of the mixing water in the cylinder.)

4) Early curing

After casting and placement in the rubber container, the specimens were stored in a 20°C climate chamber. At first, an endothermic period of about 7 hours was observed, followed by an exothermic development due to the hydration of the cement. The maximum temperature increase was 4°C.

5) Demoulding and rubber insulation

After 16 hours, the bolts were loosened from the cast-in items and the moulds removed. The specimens (both cylinders and cubes) were then insulated by a 2-mm vulcanized butyl rubber cloth. Butyl rubber cloths (where applicable) were placed at the ends of the cylinder and then removed right before testing. Clamp hoses were placed at the ends of the cylinders to avoid any moisture losses. The specimens were continuously stored in a 20°C climate chamber. After 30 hours, the temperature varied between 21 and 20°C.

3.3 Concrete mix proportions

The mix proportions were based on previous experiments of optimal proportions in HPC [5]. Concrete mix proportions are given in Table 3 in kg/m^3 of dry material, etc.).

3.4 Principal properties of the concretes

1) Compressive strength

The 28-day strength mainly depended on the so-called effective water-binder ratio, wbr_{eff}:

$$wbr_{eff} = w/(C+2\cdot S) \quad (1)$$

where w, C and S denote the water, cement and silica fume content (in kg/m^3), respectively.

The following expression was obtained for the 28-day compressive strength, fc28 (MPa):

$$fc_{28} = k_1\cdot 330\cdot(0.645 - wbr_{eff}) \quad (2)$$

Table 4 shows the effect of aggregate and air-entrainment on the compressive strength.

The strength growth rate, df_c/dt, was fairly linear logarithmic until 28 days of age (in MPa/day):

$$df_c/dt = k\cdot 14.7\cdot(2.1 - wbr_{eff}) / t \quad (3)$$

where t denotes the age (in days) and k denotes a correction factor according to Table 5.

Table 3 - Concrete mix proportions (in kg/m^3 of dry material, etc.)

Material /Type	50	90	90L	90R	110	130	130R	150
Quartzite sandstone, 8-12 mm	460							
Quartzite sandstone, 12-16 mm	460	965	930		1020	1005		1060
Natural sand, Åstorp, 0-8 mm	810	850	790		765	765		750
Granite, 12-16 mm							1065	
Pea gravel, 8-16 mm				1075				
Natural sand, Bålsta, 0-8 mm				780			770	
Cement, Degerhamn Standard	430	445	450	450	500	525	480	540
Granulated silica fume	22	45	45		50	53		54
Silica fume slurry				23			48	
Air-entraining agent, vinsole resin	0.02		0.04					
Superplasticizer (melamine formaldehyde, dry material)	2.8	5.5	4.3	5.3	4.8	6.4	7.8	9.6
Water-cement ratio	0.38	0.37	0.37	0.33	0.31	0.30	0.30	0.25
Air content (% by total volume)	4.0	0.9	4.5	0.9	0.9	0.9	0.9	1.0
Density (kg/m3)	2330	2475	2380	2480	2500	2510	2520	2540
Slump (mm)	140	160	170	145	200	230	45	45
28-day compressive strength (MPa)	89	110	92	101	127	137	122	143
1-year compressive strength (MPa)	101	124	108	115	139	144	135	162
2-year compressive strength (MPa)	112	127	121	115	145	149	131	162

Table 4 – Correction factor, k_1, in equation (2) due to mix proportion alterations

Mix proportion alteration	Mix proportion	Correction factor
Standard mix proportion	90 110, 130, 150	1.0
National aggregate	90R, 130R	0.91
Air-entrainment (≈ 4.4%)	50, 90L	0.85

Table 5 – Correction factor k in the strength growth equation (3)

Alteration	Mix proportion	Correction factor k
Standard mix proportion	90, 110, 130, 150	1.0
National aggregate	90R, 130R	0.79
Air-entrainment (≈ 4.4%)	50, 90L	0.73

Table 6 – Mix proportion correction factor, k_2, for the 28-day relative hydration, w_n/w

Alteration	Mix proportion	Correction factor
Standard	50, 90, 90L, 110, 130, 150	1.0
National aggregate	90R (4 nos.)	0.75
National aggregate	130R (4 nos.)	1.09

2) Hydration

The 28-day relative hydration, w_n/w_{28}, was obtained as a function of the effective water-binder ratio, wbr_{eff}, equation (1) (w = original content of mixing water in the concrete (in kg/m^3)):

$$w_n/w_{28} = k_2 \cdot 0.169 \cdot (2.25 - wbr_{eff}) \quad (4)$$

Table 6 shows the effect, k_2, on the 28-day relative hydration, w_n/w_{28}, of the mix proportion.

Most probably, the hydration was affected by the type of silica fume. As indicated above, silica fume slurry was used in the national mix proportions, which could be an explanation for the k_2 factor.

4. INTERNAL RELATIVE HUMIDITY

4.1 General

The most apparent and characteristic property of HPC, besides its high compressive strength, is the decline of internal relative humidity. The self-desiccation of HPC is very beneficial when solving building moisture problems for residential construction [6]. However, the self-desiccation may also be harmful. It causes the concrete to shrink even when submerged. A normal concrete shrinks only during drying when exposed to air. In HPC, an internal drying takes place due to the chemical shrinkage of the water when it is bound to the cement during the hydration process, Fig. 3 [6]. Independent of the water-cement ratio, about 1.5% of the concrete volume became gas-filled due to the chemical shrinkage. Because of the pore distribution of the concrete,

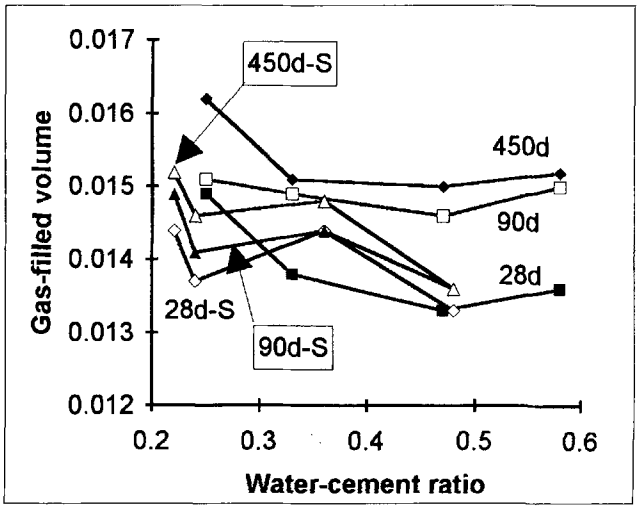

Fig. 3 – Gas-filled volume due to the chemical shrinkage of the water when it is bound to the cement during the hydration process as a function of the water-cement ratio of the concrete [6] (d = days; S = 10% silica fume).

the internal relative humidity decrease was more obvious at a lower water-cement ratio, *i.e.* for HPC. According to the well-known Kelvin equation, a concrete with pores of a smaller diameter reaches a lower internal relative humidity at the same volume of gas-filled space in the concrete (Fig. 3).

4.2 Previous research on the internal relative humidity of HPC

From studies of cement pastes [7] at different relative humidities, the β_ϕ-factor was obtained:

$$\beta_\phi = \frac{e^{B_f \cdot \phi - 1}}{e^{B_f \cdot B_\phi - 1}} \quad (5)$$

where:

β_ϕ denotes the reduction factor as a consequence of the relative humidity, ϕ,

B_f denotes a form factor,

B_ϕ denotes the value of ϕ above which $\beta_\phi = 1$.

In Fig. 4, the factor β_ϕ is given at different relative humidities ϕ [7]. Curing at low ϕ decreased the hydration considerably. The results according to Fig. 4 confirmed those obtained half a century ago [8], except for the "tail" at lower ϕ. Fig. 5 shows the internal relative humidity related to the sealed curing of large concrete elements (250 kg by weight) at 30, 90 and 450 days as a function of the effective water-binder ratio, wbr_{eff}, equation (1) [9, 10]. The results presented in Fig. 5 were obtained by measurements taken in about 150 cast-in pipes over a period of 450 days, with each measurement covering a period of 22 hours. From Fig. 5, the following water-binder ratio and time-dependent equation for self-desiccation, ϕ, was obtained:

$$\phi(wbr_{eff}, t) = 0.30 \cdot (2.2 \cdot wbr_{eff} + 2.6 - 0.1 \cdot \ln t) \quad (6)$$

where: wbr_{eff} denotes the effective water-binder ratio according to equation (1) above and t denotes the age of the concrete (days).

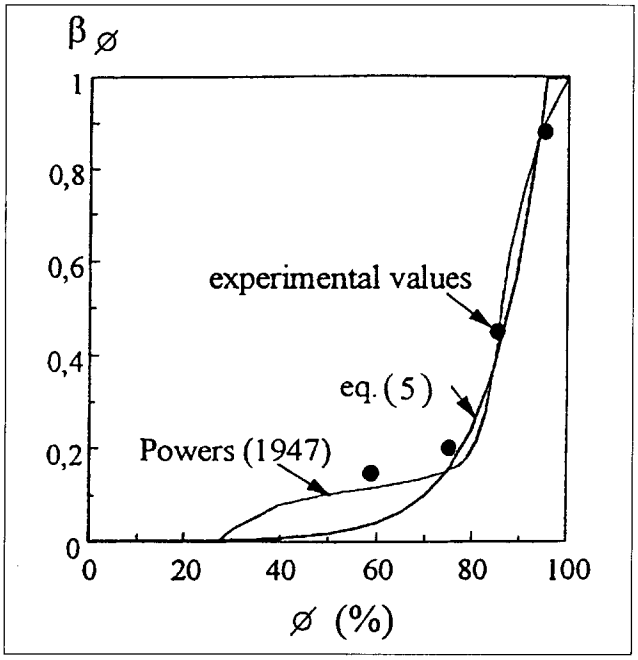

Fig. 4 – The factor β_ϕ versus the relative humidity, ϕ, for cement paste [7] ($B_f = 0.09$, $B_\phi = 96$).

4.3 Experimental methods

Immediately after the compressive strength tests had been performed, fragments of the concrete (min. 5 mm in size) were collected in 100-ml glass test tubes. The tubes were filled up to 2/3. Then they were sealed with rubber plugs. The tubes with the fragments were kept in a 20°C room. A dew point meter was used to measure the internal relative humidity, ϕ. The probe of the meter was inserted into the test tube and rubber-tightened to the glass. Since HPC contains very little moisture, the period of measurement required to obtain a stable value (equilibrium between the moisture inside the air in the pores of the concrete and the air around the sensor of the dew point meter) for ϕ was at least 12 hours. The minimum period was thus set at 16 hours [11].

4.4 Sources of error

Adopting a relative hydration of 0.50, the moisture content in the concrete was ≈ 75 kg/m^3. The air in the pores of the concrete and the air in the tube contained ≈ 0.015 kg moisture/m^3 of air. Thus, there was about 5,000 times as much moisture in the concrete as required for a moisture equilibrium between the air in the pores of the concrete and the air in the tube. The lack of moisture would thereby not constitute any source of error. Fig. 6 shows the effects of temperature on the measurement of relative humidity. A rise of 4°C caused an error in ϕ of ≈ + 0.01 [12].

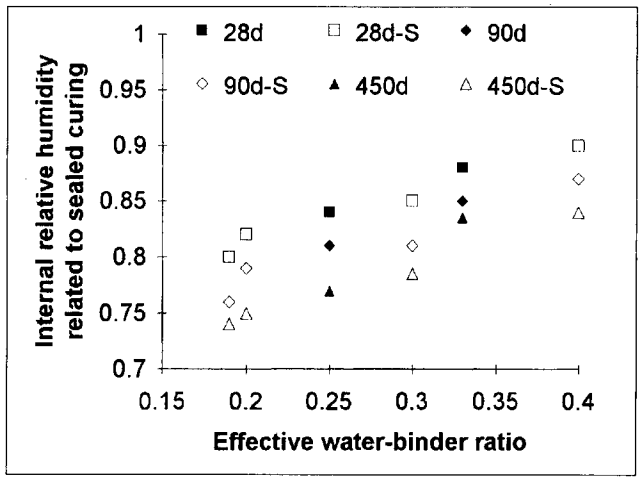

Fig. 5 – Internal relative humidity, ϕ, related to sealed curing at 30, 90 and 450 days' age as a function the effective water-binder ratio, wbr_{eff}, equation (1) [9, 10] (d = days; S = 10% silica fume).

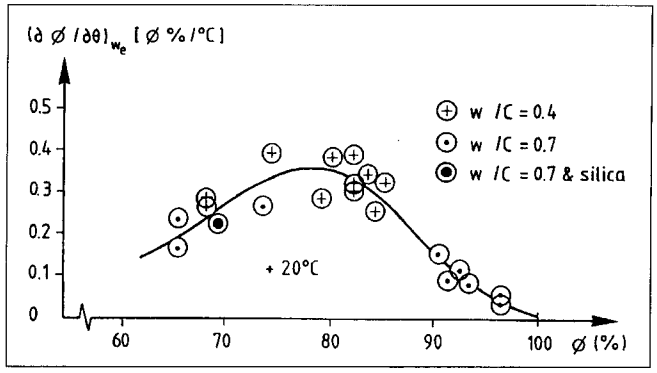

Fig. 6 – The effects of temperature on the measurements of relative humidity, ϕ [12].

4.5 Results of experiments

Fig. 7 shows the development of the internal relative humidity related to sealed curing for all the concretes tested. The type of concrete is indicated to the right of the figure. The time-dependent results are computed as the mean values of 4 tests of each concrete.

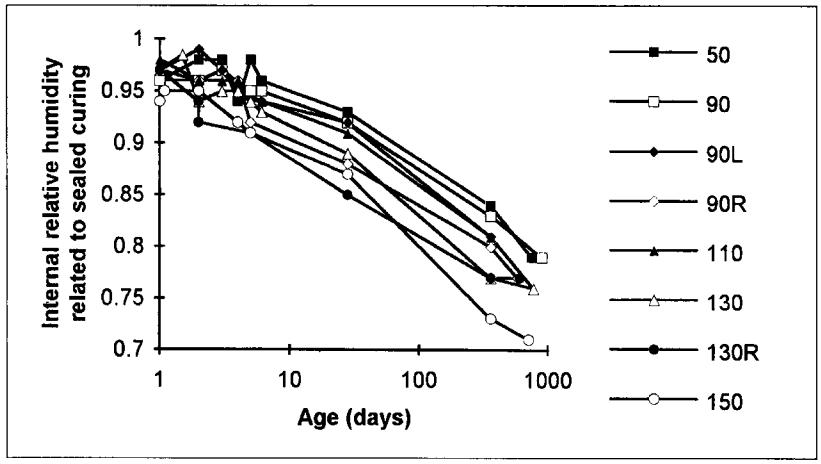

Fig. 7 – Internal relative humidity related to sealed curing. Four measurements per point [11]. The mix proportion is indicated in Table 3.

4.6 Accuracy of internal relative humidity tests

The dew point meters were salt-calibrated each month [13]. When measuring the internal relative humidity of fragments from the very same cube, some differences were noted even after the values on the display were altered according to the calibration. No systematic fault seemed to exist; some of the measured values are higher than the mean value, while some are lower. The accuracy of the measurements of internal relative humidity, ϕ, tended to be within $\pm$ 0.015 ϕ. At early ages, the total accuracy as compared to a temperature of 20°C was + 0.025, - 0.015 ϕ.

4.7 Analysis of the internal relative humidity at self-desiccation

Based upon Fig. 5, which shows the effect of silica fume on the amount of self-desiccation, the relationship between self-desiccation and the effective water-binder ratio was established (equation (6)). Fig. 8 shows the internal relative humidity, ϕ, at different ages of the concrete as a function of the effective water-binder ratio, wbr_{eff}, given in equation (1). At 5 and 28 days of age, the internal relative humidity, ϕ, at self-desiccation of the national concrete mix proportions 90R and 130R was ϕ = 0.03 and ϕ = 0.04 lower than the resisting concrete mix proportions, in keeping the effective water-cement ratio at a constant level (Fig. 8). The tendency curves in Fig. 7 were surprisingly parallel. After the initial hydration, the self-desiccation proceeded more or less independently of the water-binder ratio. The initial hydration, however, caused a drop in the internal relative humidity of ϕ = 0.08 at wbr_{eff} = 0.20 and of ϕ = 0.03 at wbr_{eff} = 0.34; thus, a difference of ϕ = 0.05. After 2 years, this difference was ϕ = 0.07 between wbr_{eff} = 0.34 (ϕ = 0.80) and wbr_{eff} = 0.20 (ϕ = 0.73).

An expression of self-desiccation was estimated at different ages:

$$\phi = g \cdot (wbr_{eff} + h) \quad (7)$$

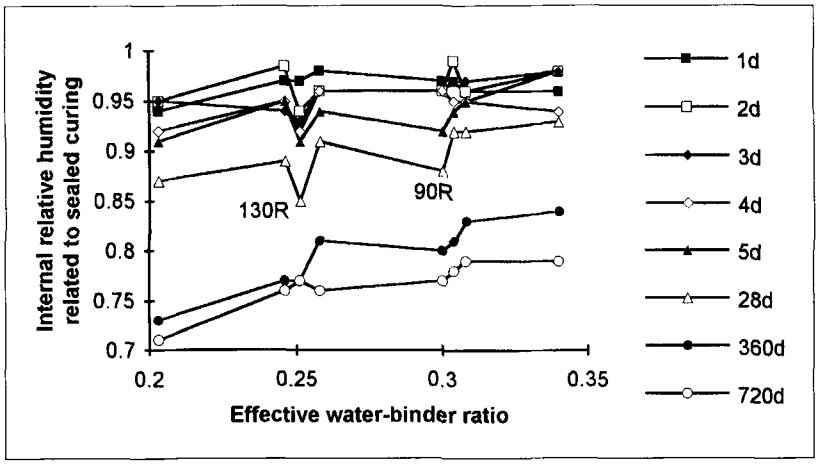

Fig. 8 – Internal relative humidity, ϕ, at self-desiccation as a function of the effective water-binder ratio, wbr_{eff}, (equation (1)) at varying ages of the concrete (d = days, R = silica fume slurry).

Table 7 – Constants g and h in equation (7)

Age	g	h	Correction of ϕ for mix proportion 90R	Correction of ϕ for mix proportion 130R
5 days	0.382	2.20	-0.03	-0.04
28 days	0.434	1.81	-0.03	-0.04
360 days	0.761	0.679	-	-
720 days	0.517	1.20	-	-

where: ϕ denotes the internal relative humidity, g and h are constants given in Table 7 and wbr_{eff} is given in equation (1) above.

Assuming a mean ϕ decrease of 0.18 between 5 days and 720 days of age, the following expression was derived for the self-desiccation (at an age of less than about 1/2 year, the corrections for national mix proportions 90R and 130R according to Table 7 apply):

$$\phi(wbr_{eff}, t) = 0.38 \cdot (wbr_{eff} + 2.4 - 0.1 \cdot \ln t) \quad (8)$$

where: wbr_{eff} denotes the effective water-binder ratio according to equation (1) and t denotes the age of concrete (in days).

The rate of self-desiccation, $d\phi/dt$, was estimated (in day^{-1}):

$$d\phi/dt = - 0.038/t \quad (9)$$

where t denotes the age of concrete (in days).

5. AUTOGENOUS SHRINKAGE

5.1 General remarks

Autogenous shrinkage has formerly been included in the basic creep by definition. The autogenous shrinkage was most probably caused by the noticeable self-desiccation of the concrete; see above. However, since the autogenous shrinkage affected the size of the basic creep, especially at early ages in combination with low loading on the specimen, its estimation had become essential [3]. The depression in the pores of the concrete caused by the self-desiccation acts as an internal force within the concrete, being restrained by the cement paste on the one hand and the aggregate in the concrete on the other. The depression in the pores occurs early during hydration according to the well-known Kelvin equation. Initially, an elastic/plastic deformation took place in the concrete, caused by the pore depression. Secondly, the force created by the depression also caused an internal creep in the concrete, mainly in the cement paste, even in those specimens not subjected to any loading at all. Thus, the aggregate is subjected to a compressive strain.

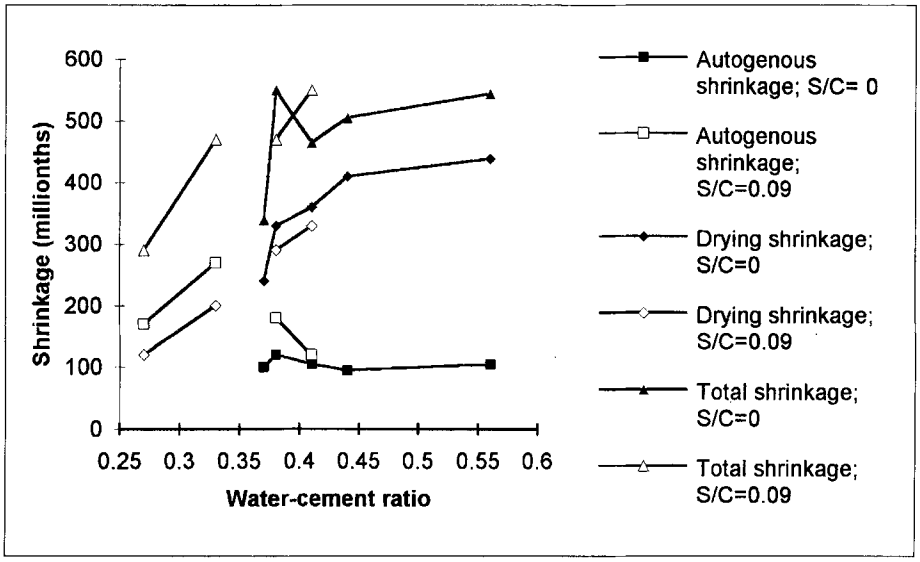

Fig. 9 – Autogenous and drying shrinkage as a function of the water-cement ratio, w/C, with different amounts of silica fume [14] (C = cement content, S = content of silica fume).

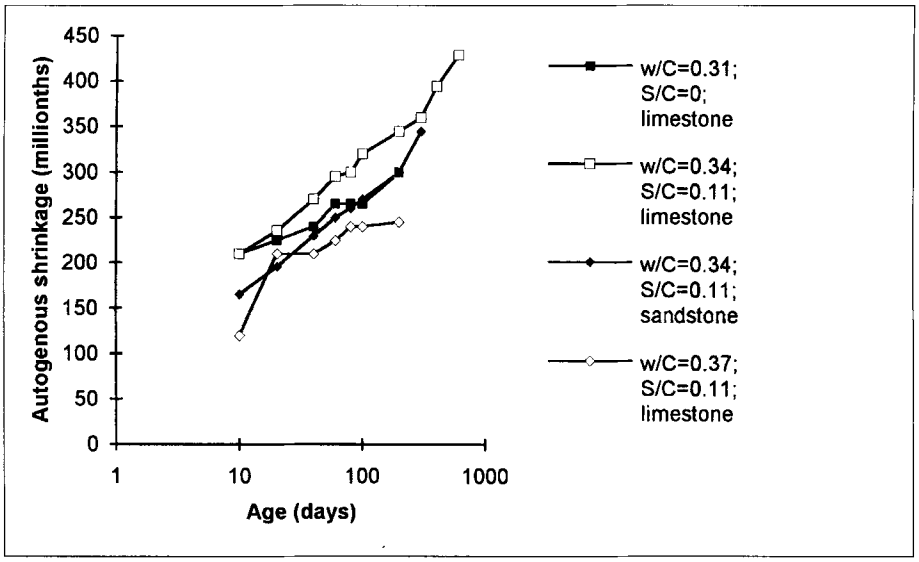

Fig. 10 – Autogenous shrinkage as a function of time. Silica fume content and water-cement ratio are indicated. Aggregate of limestone or quartzite sandstone [15] (C = cement content, S = content of silica fume, w/C = water-cement ratio).

5.2 Previous research on autogenous shrinkage

Extensive studies have been carried out on the shrinkage of both HPC and normal concrete at various water-cement ratios as well as with differing amounts of silica fume in the concrete [14]. It was found that the autogenous shrinkage increased at lower water-cement ratios. At w/C ≈ 0.30 the autogenous shrinkage after 400 days was about 230 millionths. It was also observed that the total shrinkage (drying shrinkage and autogenous shrinkage) was greater at higher water-cement ratios; for example, about 550 millionths at w/C ≈ 0.6. In Fig. 9, the results of the autogenous shrinkage and the drying shrinkage are given as a function of the water-cement ratio, w/C, with different amounts of silica fume [14].

The results in Fig. 9 were obtained for concretes with a compressive strength varying between 46 and 101 MPa. The specimen was 1 m long; its diameter was 0.16 m. The measurement of shrinkage started at ≈ 2 days of age. The following conclusions were drawn [14]:

1) The autogenous shrinkage increased with a decreasing water-cement ratio.
2) The autogenous shrinkage increased when the concrete contained silica fume.
3) The total shrinkage and the drying shrinkage both increased with an increasing water-cement ratio.

Other French experiments were carried out on 0.12-m diameter cylinders with a length of 0.24 m [15]. In this case, the water moisture losses were 1% per year of the total weight of the concrete. The measurements of shrinkage started at an age of 1.2 days. In Fig. 10, the result of the autogenous shrinkage is shown as a function of time [15]. The following conclusions were drawn [15]:

1) The autogenous shrinkage increased with a decreasing water-cement ratio.
2) The autogenous shrinkage increased in the concrete with limestone aggregate as compared to the concrete with quartzite sandstone aggregate.
3) The autogenous shrinkage was greater in concrete containing silica fume than in concrete without silica fume.

The autogenous shrinkage was studied at very early ages by cast-in strain gauges [2]. The specimen was 0.1 × 0.1 × 1.2 m. The concrete was cast in vinyl polymer plastic moulds that allow for movements of the concrete at early ages. The measurements started at ≈ 0.2 days of age. In Fig. 11, the autogenous shrinkage is indicated as a function of time for differing water-cement ratios. The autogenous shrinkage in the research conducted [2] increased with lower water-cement ratios and a lower content of silica fume, as also observed in the French experiments. The difference between autogenous and drying shrinkages was smaller with a low water-cement ratio.

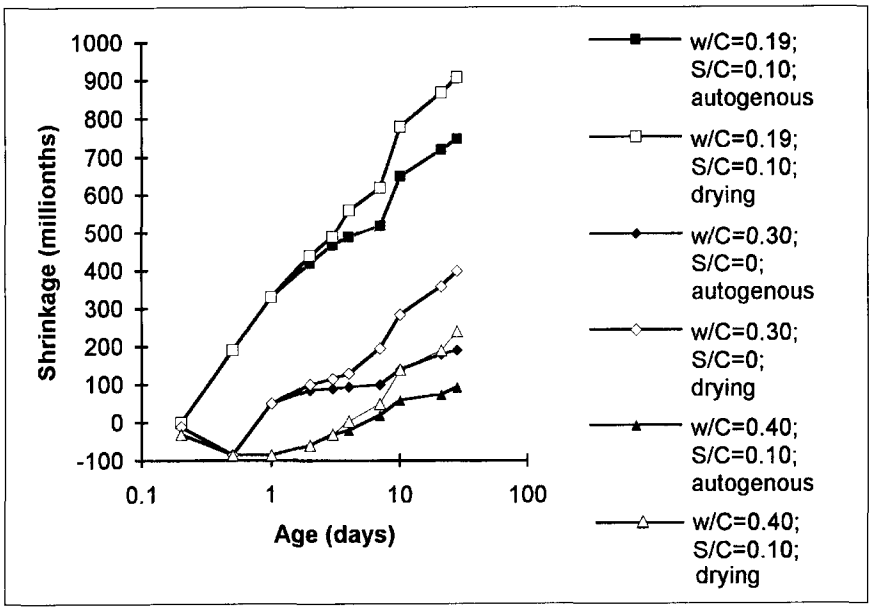

Fig. 11 – Autogenous and drying shrinkage as a function of time at different water-cement ratios [2] (C = cement content, S = content of silica fume, w/C = water-cement ratio.

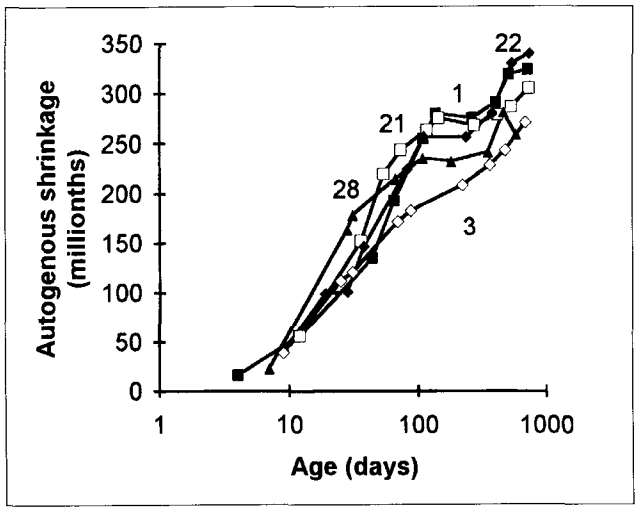

Fig. 12 – Autogenous shrinkage of 5 batches of concrete 130 as a function of the age of the concrete.

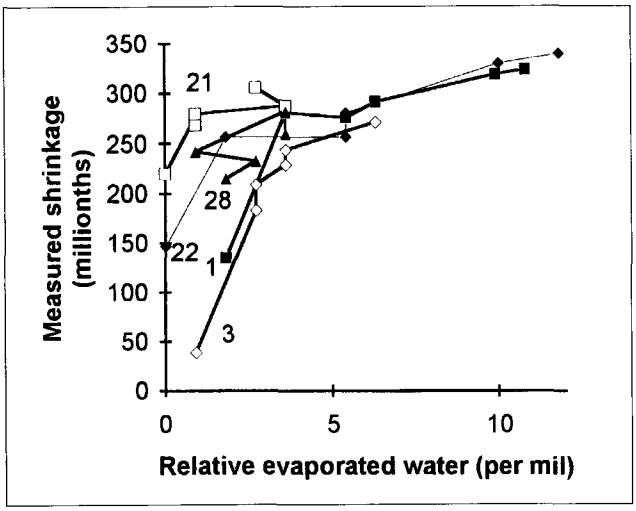

Fig. 13 – Measured shrinkage as a function of the relative evaporated water. The batch number is given.

5.3 Experimental method

In the present experiments, a total from 32 specimens cast of 8 different concretes were studied as described in Table 3. The same batches of concrete were used as in the experiments on quasi-instantaneous loading. After demoulding and insulation by butyl rubber clothing, 6 stainless steel screws were fixed into cast-in items in the cylinder. Measurements were taken on three sides of the cylinder over a length of 250 mm within 1 hour of demoulding. The specimen was then stored in a 20°C climate chamber. Gloves were used to avoid temperature effects from the contact of hands on the mechanical devices.

5.4 Sources of error

1) Moisture losses

In spite of all the careful precautions, some faults existed causing unforeseen water losses. The specimens were continuously weighed to detect this loss.

2) Moisture absorption in the insulation

Absorption of water in the butyl rubber insulation would affect the weight of the specimen.

3) Temperature movements

Temperature movements have a large effect on the measurements of the autogenous shrinkage. The effects of hydration heat, in particular, were avoided by performing the first measurement at 20°C. A thermocouple was cast in the specimen and the temperature change was monitored as the first measurement was being recorded.

4) Stability of the mechanical device

The mechanical device had been used several thousand times and might have been worn out.

5.5 Results of experiments

Fig. 12 shows a summary of the measured autogenous shrinkage of 5 batches of concrete mix proportion 130, as a function of the age of the concrete [11].

5.6 Accuracy

1) Moisture losses

In Fig. 13, the effect on the measured shrinkage of water loss due to imperfection and diffusion of the butyl rubber cloth is given for concrete 130. The relative water losses were defined as the weight losses as compared to the amount of mixing water in the concrete.

As can be observed in Fig. 13, the moisture losses for concrete 130 were small (less than 10 per mil of the mixing water over 2 years). A few specimens from other

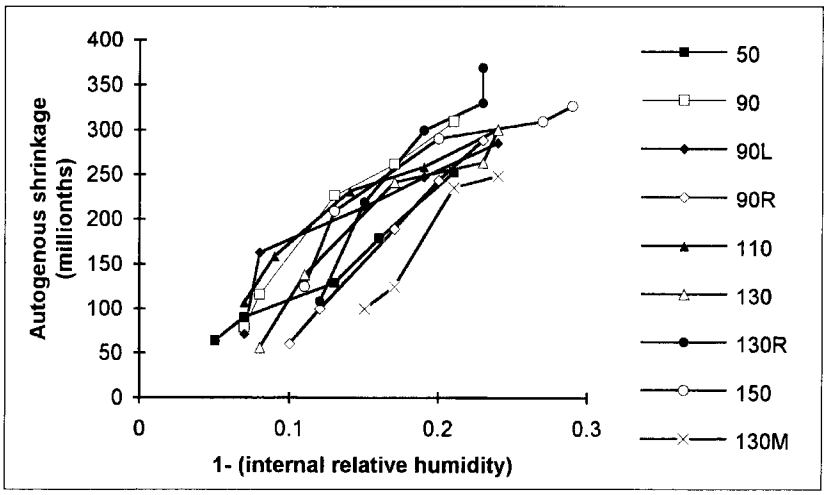

Fig. 14 – Autogenous shrinkage as a function of 1 - ϕ (ϕ = internal relative humidity). The mix proportions (given in Table 3) are indicated.

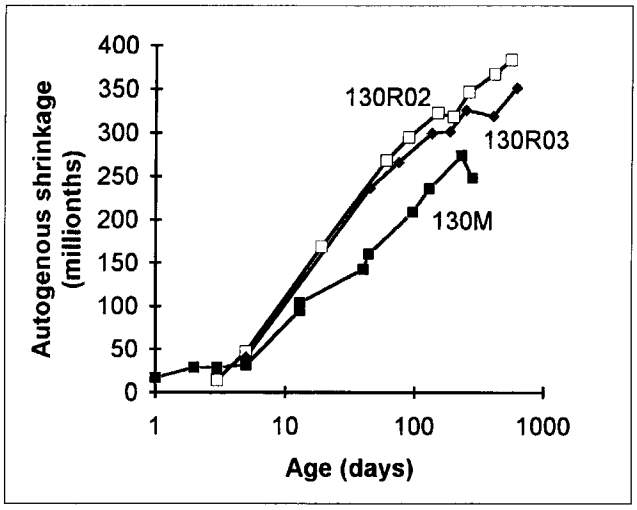

Fig. 15 – Autogenous shrinkage of concretes containing silica fume slurry (R) or granulated silica fume (M).

concretes exhibited moisture losses exceeding 10 per mil of the mixing water per year. The results of those specimens were excluded from this analysis. Twenty-five specimens thus remained to be analysed.

2) Moisture absorption in insulation

At ϕ = 0.95, the increase in the weight of a rubber insulation was hardly detectable, *i.e.* less than 0.1 g. Since the specimen contained 120 g of water, the absorption was negligible.

3) Temperature movements

A thermocouple was cast in the specimen and the temperature was monitored as the first measurement was performed. The maximum faults would then have been $4{\cdot}8{\cdot}10^{-6}$ = 32 millionths, assuming the same effect of temperature on HPC as on normal concrete. A difference of + 1°C from 20°C reduced the observed fault to ≈ + 8 millionths.

4) Stability of the mechanical devices

The mechanical devices (Huggenberger and Proceq) were continuously calibrated with an INVAR rod and with a Mitutoyo micrometer. The reading of the device probably was then within 0.002 mm, which was comparable to 10 millionths (the length of the device: 250 mm).

5) Total accuracy

The accuracy of the mechanical devices was + 0.002 mm; the measured length was 0.25 m, which yielded a fault of ≈ + 10 millionths. The total fault was then + 20 millionths, which was a fairly large fault compared to the measured total shrinkage of about 250 millionths.

5.7 Analysis

1) Effect of internal relative humidity

In Fig. 14, the autogenous shrinkage is given as a function of 1 - ϕ, with ϕ = relative humidity.

The effect of internal relative humidity, ϕ, on the autogenous shrinkage was very distinct.

2) Effect of type of silica fume

The effect of micro silica slurry on the autogenous shrinkage as compared to that of granulated silica fume is shown in Fig. 15. The mix proportions 130M and 130R were identical except for the types of silica fume (M = granulated silica fume; R = micro silica fume slurry). The water losses from all specimens in Figs. 14 and 15 were ≈ 7 per mil of the mixing water calculated on a 1-year basis. The concrete containing 10% silica slurry exhibited a slightly higher autogenous shrinkage than the concrete containing 10% granulated silica fume.

From Fig. 14, the following equations were evaluated for the autogenous shrinkage of a concrete containing 10% silica fume.

$$\varepsilon_{auR} \approx 350{\cdot}\ln(1 - \phi) + 860 \quad (10)$$

$$\varepsilon_{auM} \approx 350{\cdot}\ln(1 - \phi) + 760 \quad (11)$$

where: ε_{auR} denotes the autogenous shrinkage for concrete containing silica fume slurry (in millionths), ε_{auM} denotes the autogenous shrinkage for concrete with granulated silica fume (in millionths), ϕ denotes the internal relative humidity.

As calculated in equations (10) and (11), the concrete containing silica fume slurry exhibited about 100 millionths greater autogenous shrinkage as compared to the concrete containing granulated silica fume slurry, independent of the internal relative humidity. The reason for this phenomenon is unknown.

3) Effect of air-entrainment

In Fig. 14, the influence of air-entrainment was observed for 2 concretes, 90 and 90L, see Table 13. The same properties applied to both concretes except for the air-entrainment. As observed in Fig. 14, the development of autogenous shrinkage for the concrete containing air-entrainment was similar to that of the concrete without air-entrainment.

4) Effect of autogenous shrinkage on compliance

In Fig. 16, the autogenous shrinkage of the 25 remaining concrete specimens (as explained in Section

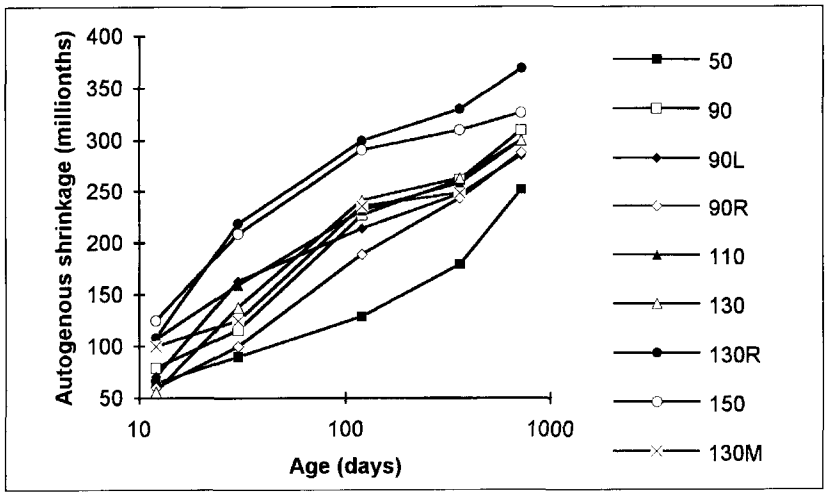

Fig. 16 – Autogenous shrinkage of 9 concretes (26 specimens) as a function of time. Mix proportions (given in Table 3) are indicated in the figure.

5.6.1 above) is given as a function of time together with the autogenous shrinkage of concrete 130M (with granulated silica fume slurry), 26 specimens in all. Fig. 16 shows the mean value of the autogenous shrinkage for each concrete mix proportion (given in Table 3).

Fig. 17 presents a summary of the autogenous shrinkage as a function of the water-cement ratio at different ages of the concrete. As can be observed in Fig. 17, the concrete with 5% silica fume exhibited about 30% less autogenous shrinkage than the concrete containing 10% silica fume. This was most probably due to the more pronounced self-desiccation in concrete with a higher silica fume content. It was also observed in Fig. 17 that the national mix proportions 90R and 130R exhibited ≈ 25% greater final autogenous shrinkage than the other mix proportions, probably due to the type of silica fume. Adopting the principle of superposition, which means that the autogenous shrinkage was included in the basic creep compliance and was dependent proportionally on the stress in the concrete only, it was possible to estimate the effect of the autogenous shrinkage on the basic creep compliance. The stresses at the quasi-instantaneous [16] loading and at the short-term loading are given in Table 8. However, the assumed principle of superposition of autogenous shrinkage and basic creep still remains to be proven by, for example, a curvature creep test method [17].

Table 8 – Concrete stress in quasi-instantaneous and in short-term loading experiments (MPa)

Concrete/Type	01	02	03	28
50	5.08	14.1	15.6	24.6
90	13.2	24	19.2	34.2
90L	9.1	21.1	14.4	27
90R	22.2	20.4	16.7	30
110	23.1	39	24.6	38.7
130	14	37.8	25.2	38.1
130R	24.9	34.8	19.9	34.9
150	27.2	34.8	24.6	40.1

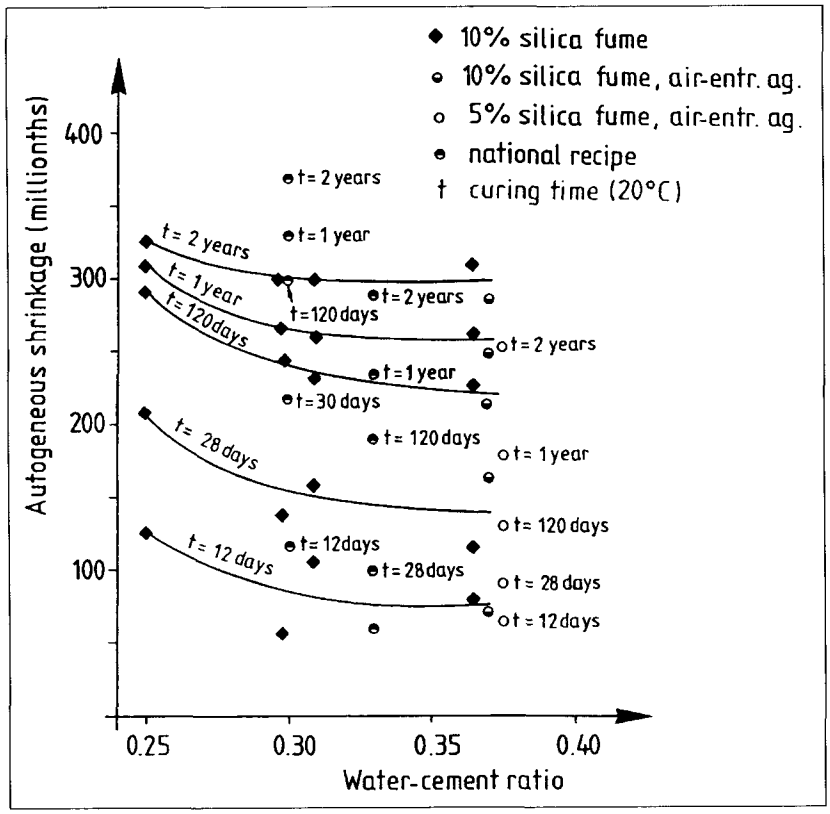

Fig. 17 – Autogenous shrinkage as a function of the water-cement ratio. The age of the concrete and the amount of silica fume and content of air-entrainment are indicated.

The following symbols are used in Table 8:

...01 Age at quasi-instantaneous loading : 0.8 days; stress/strength ratio: 0.6.

...02 Age at quasi-instantaneous loading : 2 days; stress/strength ratio: 0.6.

...03 Age at quasi-instantaneous loading : 2 days; stress/strength ratio: 0.3.

...28 Age at quasi-instantaneous loading : 28 days; stress/strength ratio: 0.3.

As an example, if autogenous shrinkage is not reduced from the creep strain, the effect on compliance will be $\Delta J(t,t')$ (in millionths/MPa):

$$\Delta J(t,t') = \varepsilon_{aut'}/\sigma \qquad (12)$$

t denotes the age of the concrete (days),

t′ denotes the age of the concrete at loading (days),

t - t′ denotes the loading time (days),

$\varepsilon_{aut'}$ denotes the autogenous shrinkage of the concrete after loading (millionths),

σ denotes the constant stress used during the creep tests, see Table 8 (MPa).

The effect of autogenous shrinkage on the compliance of mature concrete was minor, about 5 millionths/MPa after 2 years of loading. However, when the loading was applied at early ages, the fault of the autogenous shrinkage on the compliance was much greater. After 2 years of constant loading, the effect varied between 12 millionths/MPa (concrete type 150) and 50 millionths/MPa (concrete type 50). For further calculations, it was essential to obtain a model of the effect of autogenous shrinkage on the compliance. In Fig. 18, the effect of autogenous shrinkage on the compliance after 2 years of loading is given as a function of the ratio of the stress and the 28-day strength of the concrete. The concrete containing 5% silica fume powder is indicated separately (mix proportion 50). The national mix proportion concretes are also indicated in Fig. 18 (90R and 130R). The two following general equations were derived for the effect of autogenous shrinkage on compliance, $\Delta J(t,t', \omega)$ (in millionths/MPa):

$$\Delta J(t,t', \omega) = 16 \cdot (0.35 - \omega) \cdot \ln(t - t') \quad (13)$$

$$\Delta J(t,t', \omega) = 9.2 \cdot \ln(t - t') \cdot e^{-7.4\omega} \quad (14)$$

where:

t denotes the age of the concrete (days),
t' denotes the age of the concrete at loading (days),
$t - t'$ denotes the loading time (days),
ω denotes the stress/28-day strength ratio, σ/f_{c28},
σ denotes the stress used during the creep tests, see Table 8 (MPa),
f_{c28} denotes the 28-day strength of the concrete (MPa).

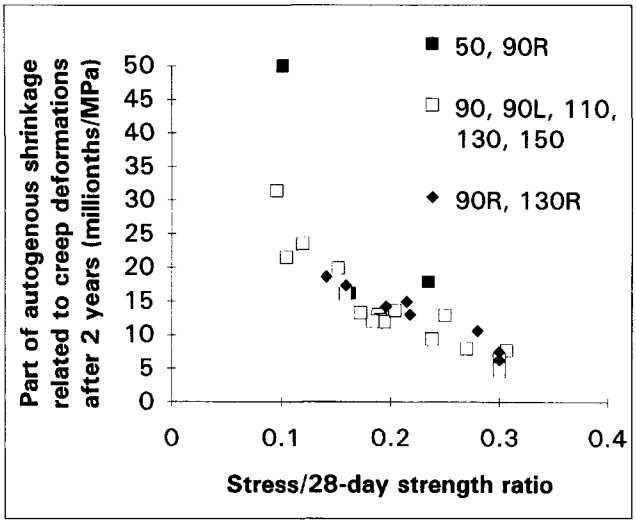

Fig. 18 – The effect on compliance of autogenous shrinkage after 2 years of loading as a function of the ratio of the stress to the 28-day strength, σ/f_{c28}. The type of concrete is indicated.

5) Models of autogenous shrinkage

As described above, the self-desiccation of the HPC was the fundamental precondition for the autogenous shrinkage to occur. The time-dependence and the relationship to the water-cement ratio of the relative humidity, ϕ, were known from equation (8) above. The autogenous shrinkage for concrete containing 10% silica fume slurry (R) was estimated according to equation (10):

$$\varepsilon_{auR} \approx 350 \cdot \ln(1 - \phi) + 860 \quad (10)$$

Fig. 14 yielded the autogenous shrinkage for concrete with 5% silica fume, ε_{au5}, (millionths):

$$\varepsilon_{au5} \approx 1320 \cdot (0.98 - \phi) \quad (15)$$

The concretes with 10% granulated silica fume 90, 90L, 110, 130 and 150 exhibited the following autogenous shrinkage, ε_{aur} (millionths):

$$\varepsilon_{aur} = 170 \cdot \ln(1 - \phi) + 550 \quad (16)$$

where:

ε_{auR} denotes the autogenous shrinkage for concrete containing 10% silica fume slurry (millionths),
ε_{aur} denotes the autogenous shrinkage for concrete with 10% granulated silica fume (millionths),
ε_{au5} denotes the autogenous shrinkage for concrete with 5% granulated silica fume (millionths),
ϕ denotes the internal relative humidity.

6. CONCLUSIONS

This article began by presenting the general objectives and layout of the work. A summary was provided of the present state knowledge of self-desiccation and autogenous shrinkage of concrete. In the original experimental results presented in this article, the self-desiccation and autogenous shrinkage were studied on more than 300 cubes and 30 cylinders. The principal results obtained were:

1) The self-desiccation, ϕ, depended on the age of the concrete, the water-cement ratio and the silica fume content. At early ages, *i.e.* at less than 28 days, the type of silica fume also affected the amount of self-desiccation.
2) The autogenous shrinkage mainly depended on the self-desiccation, ϕ, of the concrete.
3) At a constant water-cement ratio and with 10% silica fume (calculated on the cement content), the autogenous shrinkage was greater when silica fume slurry was used than when granulated silica fume was used in the concrete.
4) At a constant water-cement ratio, a lower autogenous shrinkage was obtained with 5% silica fume than with 10% silica fume (calculated on the cement content).
5) No influence of air-entrainment on the autogenous shrinkage was observed.
6) If the autogenous shrinkage was not reduced from the creep strain, the effect on the compliance was dependent on the ratio of the stress and on the 28-day strength of the concretes.

ACKNOWLEDGEMENTS

Financial support from the Swedish-Norwegian Consortium of High Performance Concrete (BFR, Cementa, Elkem, Euroc Beton, NCC Bygg, NUTEK,

SKANSKA and Strängbetong) along with their permission for the publication of these results are gratefully acknowledged. I am also most grateful to Professor Dr. Göran Fagerlund at Lund Institute of Technology, Division of Building Materials, University of Lund, Lund, Sweden for his critical review.

REFERENCES

[1] Bažant, Z.P. and Carol, I., 'Preliminary guidelines and recommendations for characterising creep and shrinkage in structural design codes', in Proceedings of the Fifth international RILEM Symposium in Barcelona, 1993 (E&FN Spon. London, 1993) 805-829.

[2] Tazawa, E. and Miyazawa, S., 'Autogenous shrinkage of concrete and its importance in concrete technology', *Ibid.* 159-168.

[3] Acker, P., 'Recommendations for measurement of time-dependent strains of concrete loaded in compression', *Ibid.* 849-858.

[4] Hassanzadeh, M., 'Fracture mechanical properties', Report M4:05, The Consortium of High Performance Concrete' (CBI Stockholm, 1994) 8-13.

[5] Persson, B., 'Hydration, structure and strength of high performance concrete' Report TVBM-1009 (Lund Institute of Technology, Division of Building Materials, Lund, 1992) 75-97; 351-354.

[6] Persson, B., 'Self-desiccating high-strength concrete slabs', in 'Proceedings of the Symposium on High-Strength Concrete' in Lillehammer, Norway 1993 (Edited by Holand and Sellevold) 882-889.

[7] Norling Mjörnell, K., 'Self-desiccation in concrete', Report P-94:2 (Division of Building Materials, Chalmers University of Technology, Gothenburg, 1993) 21-28.

[8] Powers, T.C. and Brownyard, T.L., 'Studies of Physical Properties of Hardened Portland Cement Paste' (Research Laboratories PCA, Bulletin 22, 1946-1948) 473-488.

[9] Persson, B. 'Hydration, structure and strength of high performance concrete, Laboratory data and calculations', Report TVBM-7011 (Lund Institute of Technology, Division of Building Materials, Lund, 1992) 83-92.

[10] Persson, B., 'Hydration, structure and strength of high performance concrete', Report TVBM-1009 (*Ibid.*, 1992) 99-123.

[11] Persson, B., 'Basic Creep of High Performance Concrete', The Consortium of High Performance Concrete (*Ibid.*, 1995) 38-46; 74-87.

[12] Nilsson, N.O., 'Temperature effects in relative humidity measurements on concrete - some preliminary studies', The Moisture Research Group Informs, Report 1987:1 (The Swedish Council of Building Research, Stockholm, 1987) 84.

[13] ASTM E 104-85, 'Standard Practice for Maintaining Constant Relative Humidity by Means of Aqueous Solutions' (The American Society for Testing and Materials, Philadelphia, 1985) 33-34, 637.

[14] le Roy, R. and de Larrard, F., 'Creep and shrinkage of high-strength concrete', in 'Proceedings of the Fifth International RILEM Symposium in Barcelona, 1993' (E&FN Spon. London, 1993) 500-508.

[15] Sicard, V., 'Origines et propriétés des déformations de retrait et de fluage des bétons à hautes performances à partir de 28 heures de durcissement' (Laboratoire Matériaux et Durabilité de Constructions, INSA-UPS no. 201, Toulouse, 1993) 55-81.

[16] Acker, P., 'Creep and shrinkage of concrete', in 'Proceedings of the Fifth International RILEM Symposium in Barcelona, 1993' (E&FN Spon, London, 1993) 7-14.

[17] Bažant, Z.P. and Xi, Y., 'New test method to separate microcracking from drying creep: curvature creep at equal bending moments and various axial forces', *Ibid.*, 77-82.